Ab Initio Calculations of the Ring Opening of Methylenecyclopropane Radical Cation to Trimethylenemethane Radical Cation

Ping Du and Weston Thatcher Borden*

Contribution from the Department of Chemistry, University of Washington, Seattle, Washington 98195. *Received March 3, 1987*

Abstract: Ab initio calculations find that ring opening of both the $^2B_1$ π and $^2A_1$ σ states of methylenecyclopropane radical cation ($MCP^{\bullet+}$) to trimethylenemethane radical cation ($TMM^{\bullet+}$) is exothermic. Disrotation is computed to be preferred to conrotation for ring opening of both states. The calculations show that disrotatory ring opening should require an activation energy of about 2 kcal/mol for $^2B_1$ but should proceed without a barrier for $^2A_1$. $TMM^{\bullet+}$ is predicted to prefer a planar geometry, and pseudorotation between $^2B_1$ minima, via $^2A_2$ transition states, is computed to be very facile. The experimental data on $MCP^{\bullet+}$ derivatives **5** and **6** are discussed in light of the computational results on ring opening of the parent $MCP^{\bullet+}$.

Although EPR evidence for the ring opening of cyclopropane radical cation (**1**) to trimethylene radical cation (**2**) has been obtained,[1] ab initio calculations have cast doubt on this interpretation of the EPR spectra.[2,3] Not only is **2** computed to be considerably higher in energy than **1**,[2] but **2** is also calculated to undergo rearrangement to propenyl radical cation with little or no activation.[3] The computational results thus indicate that **2** is not a stable intermediate on the $C_3H_6^{\bullet+}$ potential surface and, therefore, should not be observable. Other interpretations of the EPR spectrum ascribed to **2** have been offered.[1c,2]

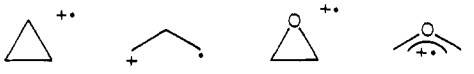

1 **2** **3** **4**

In contrast, the EPR evidence[4] that the oxirane radical cation (**3**) undergoes irreversible ring opening to the carbonylylide radical cation (**4**) has found support from ab initio calculations which show the ring opening to be exothermic and to require only a small activation energy.[5] Stabilization of **4** by delocalization of the π lone pair of electrons on oxygen[6] is presumably responsible for the fact that opening of **3** to **4** is computed to be exothermic, whereas, opening of **1** to **2** is calculated to be quite endothermic.

Methylenecyclopropane is also an obvious candidate for undergoing thermodynamically favorable ring opening upon removal of an electron from the bond between C-2 and C-3. The additional ring strain due to the trigonal carbon at C-1[7] should favor ring opening, as should the electron delocalization possible in the resulting trimethylenemethane radical cation. Indeed, Miyashi and co-workers have reported chemical[8] and spectroscopic[9] evidence for ring opening on electron transfer from 2,2-diarylmethylenecyclopropanes (**5**).

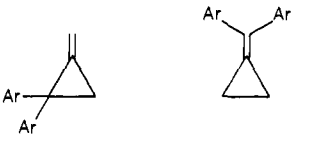

5 **6**

In contrast, with a pair of aryl groups on the double bond of methylenecyclopropane (**6**), ring opening does not occur upon electron transfer to form the radical cation.[9] A possible explanation for this difference between **5** and **6** is that ionization of **5** occurs from an orbital which contributes to the σ bond between C-2 and C-3 of the cyclopropane ring, whereas, ionization of **6** involves removal of a π electron. Consistent with this explanation is the fact that the photoelectron spectrum of the parent methylenecyclopropane shows low-energy bands corresponding to removal of both σ and π electrons.[10] Consequently, a difference in the nature of the ground state of the radical cation formed from **5** and that formed from **6** is certainly conceivable.

The explanation proposed above for the difference between the behavior of **5** and **6** upon ionization raises the question of which state or states of the parent methylenecyclopropane radical cation ($MCP^{\bullet+}$) can be expected to undergo ring opening to the trimethylenemethane radical cation ($TMM^{\bullet+}$). Since TMM possesses a degenerate (e″) pair of MOs at D_{3h} geometries, two low-lying states of the radical cation, $^2A_2$ and $^2B_1$, can be formed, depending on which of the degenerate MOs is occupied. The two lowest lying states of the radical cation are given C_{2v} rather than D_{3h} symmetry labels because the Jahn-Teller theorem[11] predicts that the equilibrium geometry of $TMM^{\bullet+}$ will have at most C_{2v} symmetry.

Correlation diagrams show that both the $^2A_1$ σ and the $^2B_1$ π states of $MCP^{\bullet+}$ can undergo orbital symmetry allowed[12] disro-

(1) (a) Qin, X.-Z.; Williams, F. *Chem. Phys. Lett.* **1984**, *112*, 89. (b) Williams and co-workers [Qin, X.-Z.; Snow, L. D.; Williams, F. *J. Am. Chem. Soc.* **1984**, *106*, 7640] have also obtained EPR evidence for ring opening of tetramethylcyclopropane radical cation in $CFCl_2CF_2Cl$ matrices. Ring opening of the parent radical cation was first questioned by Symons. [(c) Symons, M. C. R. *Chem. Phys. Lett.* **1985**, *117*, 381], who suggested nucleophilic complexation of the cationic center. This suggestion has been discussed by Williams et al. [(d) Qin, X.-Z.; Snow, L. D.; Williams, F. *Chem. Phys. Lett.* **1985**, *117*, 383. (e) Qin, X.-Z.; Williams, F. *Tetrahedron* **1986**, *42*, 6301].

(2) (a) Wayner, D. D. M.; Boyd, R. J.; Arnold, D. R. *Can. J. Chem.* **1985**, *63*, 3283. (b) Hrovat, D. A.; Du, P.; Borden, W. T. *Chem. Phys. Lett.* **1986**, *123*, 337.

(3) Du, P.; Hrovat, D. A.; Borden, W. T., submitted for publication in *J. Am. Chem. Soc.*

(4) (a) Snow, L. D.; Wang, J. T.; Williams, F. *Chem. Phys. Lett.* **1983**, *100*, 193. (b) Qin, X.-Z.; Snow, L. D.; Williams, F. *J. Am. Chem. Soc.* **1985**, *107*, 3366. See also: (c) Bally, T.; Nitsche, S.; Haselbach, E. *Helv. Chim. Acta* **1984**, *67*, 86.

(5) (a) Clark, T. *J. Chem. Soc., Chem. Commun.* **1984**, 666. (b) Nobes, R. H.; Bouma, W. J.; MacLeod, J. K.; Radom, L. *Chem. Phys. Lett.* **1987**, *135*, 78.

(6) The question of whether or not the lone pair is symmetrically delocalized in the carbonyl ylide radical cation has been addressed by ab initio calculations, which show a flat potential surface for bond length distortions from C_{2v} symmetry and a small energy requirement for twisting one methylene group out of conjugation: (a) Feller, D.; Davidson, E. R.; Borden, W. T. *J. Am. Chem. Soc.* **1984**, *106*, 2513. (b) Bouma, W. J.; Poppinger, D.; Saebo, S.; MacLeod, J. K.; Radom, L. *Chem. Phys. Lett.* **1984**, *104*, 198. The EPR spectrum of the carbonylylide radical cation is consistent with a fully delocalized species,[4] except in a $CFCl_2CF_2Cl$ matrix. (c) Qin, X.-Z.; Snow, L. D.; Williams, F. *J. Phys. Chem.* **1985**, *89*, 3602. It should be noted, however, that it is also only in this matrix that observation of a localized trimethylene radical cation has been claimed.[1]

(7) Wiberg, K. B.; Fenoglio, R. A. *J. Am. Chem. Soc.* **1968**, *90*, 3395.

(8) (a) Takahashi, Y.; Miyashi, T.; Mukai, T. *J. Am. Chem. Soc.* **1983**, *105*, 6511. (b) Miyashi, T.; Kamata, M.; Mukai, T. *Ibid.* **1986**, *108*, 2755.

(9) Miyashi, T.; Takahashi, Y.; Mukai, T.; Roth, H. D.; Schilling, M. L. M. *J. Am. Chem. Soc.* **1985**, *107*, 1079.

(10) Bieri, G.; Burger, F.; Heilbronner, E.; Maier, J. P. *Helv. Chim. Acta* **1977**, *60*, 2213.

(11) Jahn, H. A.; Teller, E. *Proc. R. Soc. London, Ser. A* **1937**, *161*, 220.

0002-7863/87/1509-5330$01.50/0

Table I. UHF-Optimized 6-31G* Geometries of MCP and Low-Lying States of $MCP^{\bullet+}$ [a]

state	R_1 [b]	R_2	R_3	r_1 [b]	r_2	a_1 [c]	a_2	β
MCP $^1A_1$	1.308	1.462	1.527	1.076	1.077	117.1	114.3	27.8
$MCP^{\bullet+}$ $^2B_1$	1.398	1.450	1.517	1.075	1.079	119.3	114.7	32.6
$MCP^{\bullet+}$ $^2A_1$	1.317	1.456	1.971	1.073	1.077	118.3	117.9	−3.0
$MCP^{\bullet+}$ $^2B_2$	1.299	1.616	1.425	1.079	1.077	118.4	118.1	49.5

[a] See Figure 1 for definition of geometrical parameters. [b] Bond lengths in Å. [c] Bond angles in degrees.

tatory ring opening to the $^2B_1$ state of $TMM^{\bullet+}$, provided that both of these C_{2v} states of $MCP^{\bullet+}$ lie on the global potential surface of lowest energy. In the disrotatory mode of ring opening only the symmetry plane perpendicular to the ring is preserved, and $^2A_1$ and $^2B_1$ of $MCP^{\bullet+}$ and $^2B_1$ of $TMM^{\bullet+}$ are all symmetric with respect to this plane. If, at the optimal C_{2v} geometry of $^2A_1$ and of $^2B_1$, each is the $MCP^{\bullet+}$ state of lowest energy, then both lie on the same $^2A'$ potential surface in the C_s symmetry that is maintained during disrotatory ring opening.[13] Hence, both can undergo symmetry-allowed ring opening to the $^2B_1$ state of $TMM^{\bullet+}$, which also lies on this potential surface.

The $^2A_1$ σ state of $MCP^{\bullet+}$, in which the singly occupied ring orbital is largely localized between C-2 and C-3,[14] also correlates with $^2A_2$ of $TMM^{\bullet+}$ via a conrotatory pathway. Among the goals of the computational research described in this paper was the determination of which mode of ring opening is preferred for the σ state of $MCP^{\bullet+}$, whether ring opening from either the σ or π state of $MCP^{\bullet+}$ is thermodynamically favorable, and whether ring opening from either state is kinetically inhibited by a substantial activation energy.

The photoelectron spectrum of MCP indicates that the $^2B_1$ π state of the radical cation is lowest in energy,[10] but the energy ordering of the states in $TMM^{\bullet+}$ is uncertain. Although $^2A_2$ and $^2B_1$ of $TMM^{\bullet+}$ form the two components of a degenerate $^2E''$ state at D_{3h} geometries and although the first-order energy lowering of each on distortion from D_{3h} symmetry must be the same, higher order effects can cause the energies of these two states to differ at their equilibrium geometries.[15] Another goal of this research was to determine the relative energies of these two states and, hence, the topography of the potential surface for pseudorotation[15] in planar $TMM^{\bullet+}$.

Numerous theoretical and experimental studies of neutral TMM agree that, unlike the triplet ground state, which prefers a planar geometry, the lowest singlet state has one methylene group twisted out of conjugation.[16] This has been shown to result from minimization of the Coulombic repulsion energy between the nonbonding electrons in the singlet. Since $TMM^{\bullet+}$ has only one nonbonding electron, one might therefore anticipate that both $^2A_2$ and $^2B_1$ of the radical cation would prefer planar geometries. Nevertheless, a twisted geometry for the substituted methylene group in the $TMM^{\bullet+}$ radical cation formed from **5** has been suggested as a possible explanation of the observation that back electron transfer to this radical cation does not produce any **6**.[8,9] Thus, a further goal of this computational study was to determine the energetic cost, if any, of twisting one methylene group out of conjugation in both low-lying states of $TMM^{\bullet+}$.

Results and Discussion

The lowest energy bands in the photoelectron spectrum of MCP, in order of increasing energy, have been assigned to formation of the $^2B_1$, $^2B_2$, and $^2A_1$ states of $MCP^{\bullet+}$.[10] $^2B_1$ is the lowest π state; $^2B_2$ is a σ state, formed by removing an electron from the antisymmetric combination of equivalent C–C ring bonds.[14] $^2A_1$ is also a σ state, formed by removing an electron from a ring orbital that is largely localized between C-2 and C-3.[14] We began by calculating the relative energies of these three states of $MCP^{\bullet+}$.

Table II. Relative Energies of the Low-Lying Electronic States of $MCP^{\bullet+}$ at the UHF-Optimized 6-31G* Geometry for MCP

state	UHF [a]	MP_2 [a]	RHF [b]	SD–CI [b]	experiment
$^2B_1$	−154.5843 [c]	−155.0445 [c]	−154.5962 [c]	−155.0310 [c]	0
$^2B_2$	1.46 [d]	0.96 [d]	1.54 [d]	1.10 [d]	0.9 [d]
$^2A_1$	1.76	1.44	1.80	1.53	1.7

[a] 6-31G* basis set. [b] Dunning SVP basis set. [c] Energy in hartrees. [d] Energy, relative to $^2B_1$, in eV.[10]

Table III. Relative Energies of the Low-Lying Electronic States of Planar and Twisted $TMM^{\bullet+}$, of $MCP^{\bullet+}$, and of the Transition States Connecting $TMM^{\bullet+}$ with $MCP^{\bullet+}$

state	UHF [a]	MP2 [a]	RHF [b]	SD–CI [b]
planar $TMM^{\bullet+}$ $^2B_1$	−154.6095 [c]	−155.0659 [c]	−154.6185 [c]	−155.0528 [c]
planar $TMM^{\bullet+}$ $^2A_2$	−6.6 [d]	5.5 [d]	8.3 [d]	2.7 [d]
twisted $TMM^{\bullet+}$ $^2B_2$	5.2	6.4	2.9	5.4
twisted $TMM^{\bullet+}$ $^2A_2$	22.3	37.4	33.4	30.2
$MCP^{\bullet+}$ $^2B_1$	9.7	6.6	7.4	6.5
$MCP^{\bullet+}$ $^2A_1$	20.8	18.7	20.7	17.0
$MCP^{\bullet+}$ $^2B_2$	24.3	17.5	23.6	16.9
conrotatory TS	25.9	23.0	26.3	20.3
disrotatory TS	19.3	8.2	18.5	10.6

[a] 6-31G* basis set. [b] Dunning SVP basis set. [c] Energy in hartrees. [d] Energy, relative to $^2B_1$ of planar $TMM^{\bullet+}$, in kcal/mol.

First, we computed their energies at the optimized geometry of MCP, so that the relative energies calculated could be compared with the vertical ionization potentials of 9.6, 10.5, and 11.3 eV measured for MCP. Like the rest of the geometries reported in this paper, the structure of MCP was optimized with the 6-31G* basis set,[17] using Gaussian 82.[18] The optimized SCF geometry (E = −154.8873 hartrees) is given in Table I.

The energies of the three low-lying states of $MCP^{\bullet+}$ were computed at this geometry, using UHF wave functions. The energies were also calculated with second-order Møller–Plesset (MP2) perturbation theory.[19] In addition to the UHF and MP2 calculations with the 6-31G* basis set, RHF and CI calculations were performed with the Dunning split-valence basis set, which was augmented by a set of polarization functions on carbon.[20] The RHF and CI calculations with this SVP basis set were carried out with MELD.[21]

The CI calculations involved all single and double excitations from the RHF configuration. The SD excitations generated 113 774 spin-adapted configurations for $^2B_1$, 112 249 for $^2B_2$, and 112 161 for $^2A_1$. Perturbation theory was used to select the energetically most important of these for each state, and CI calculations were performed for approximately 25 000 of these configurations. These CI calculations led to the variational recovery of more than 90% of the correlation energy, predicted by perturbation theory, for each state. The ratio of each CI energy to that obtained by second-order perturbation theory for the same configurations was used to scale the second-order perturbation energy calculated for the wave function involving all the SD excited configurations. The resulting estimated SD–CI energy for each state is reported in Table II along with the UHF, MP2, and RHF energies.

(12) Woodward, R. B.; Hoffmann, R. *Angew. Chem., Int. Ed. Engl.* **1969**, *11*, 781.

(13) In going from the optimal geometry of $^2A_1$ to the optimal geometry of $^2B_1$ along a pathway that maintains C_{2v} symmetry, these two states cross. However, in C_s symmetry both wave functions are $^2A'$; and, consequently, they mix, so that the crossing becomes avoided. The $^2A_1$ and $^2B_1$ minima both lie on the lower energy of the two potential surfaces which result from the avoided crossing.

(14) This MO is depicted in: Jorgensen, W. L.; Salem, L. *The Organic Chemist's Book of Orbitals*; Academic: New York, 1973, p 196.

(15) Davidson, E. R.; Borden, W. T. *J. Chem. Phys.* **1983**, *87*, 4783.

(16) Review: Borden, W. T. In *Diradicals*; Borden, W. T., Ed.; Wiley: New York, 1982; pp 24–36.

(17) Hariharan, P. C.; Pople, J. A. *Theor. Chim. Acta* **1973**, *28*, 212.

(18) Binkley, J. S.; Frisch, M. J.; Raghavachari, M.; Fluder, E.; Seeger, R.; Pople, J. A., Carnegie–Mellon University.

(19) (a) Møller, C.; Plesset, M. S. *Phys. Rev.* **1936**, *46*, 618. (b) Pople, J. A.; Binkley, J. S.; Seeger, R. *Int. J. Quantum Chem.* **1976**, *S10*, 1.

(20) Dunning, T. H.; Hay, P. J. In *Methods of Electronic Structure Theory*; Schaefer, H. F., III, Ed.; Plenum: New York, 1977; Vol. 2.

(21) Developed by E. R. Davidson and co-workers at the University of Washington.

Table IV. UHF-Optimized 6-31G* Geometries for Low-Lying States of Planar and Twisted $TMM^{\bullet+}$ [a]

state	R_1 [b]	R_2	r_1 [b]	r_2	r_3	a_1 [c]	a_2	a_3	a_4
planar $^2B_1$ [d]	1.454	1.422	1.072	1.076	1.074	119.1	115.4	121.7	121.6
planar $^2A_2$ [d]	1.414	1.440	1.075	1.073	1.073	117.3	124.7	120.7	121.0
twisted $^2B_2$	1.486	1.379	1.073	1.076	1.075	120.0	114.6	121.5	121.7
twisted $^2A_2$	1.463	1.396	1.081	1.074	1.073	116.8	127.2	123.3	118.7

[a] See Figure 2 for definition of geometrical parameters. [b] Bond lengths in Å. [c] Bond angles in degrees. [d] C–C bond lengths and C–C–C bond angles optimized with ASSEFAPC CI with the Dunning SV basis set.

Inspection of Table II shows that at all levels of theory the agreement of the calculated with the measured vertical energy differences between the low-lying states of $MCP^{\bullet+}$ is good. However, the MP2 and SD–CI calculations, which include rather extensive electron correlation, give somewhat better relative energies for $^2B_2$ than do the UHF and RHF calculations. At all levels of theory $^2B_2$ is the vertical σ state of lowest energy.

The geometry of each of these three states was then optimized separately in C_{2v} symmetry, and the adiabatic energies were computed. The optimized structures are given in Table I, and their energies are contained in Table III. The large amount of geometrical relaxation possible by stretching the bond between C-2 and C-3 in the $^2A_1$ σ state results in its adiabatic energy being calculated as almost the same as that of $^2B_2$.

As discussed above, both the $^2A_1$ σ state and the $^2B_1$ π state of $MCP^{\bullet+}$ correlate with low-lying states of $TMM^{\bullet+}$. Therefore, UHF vibrational analyses were performed on the optimized C_{2v} structures for these two states of $MCP^{\bullet+}$ to see if either would be found to open spontaneously to $TMM^{\bullet+}$. The vibrational analyses were carried out with the smaller 3-21G basis set[22] at geometries optimized with this basis set.

The $^2A_1$ σ state was found to have one imaginary vibrational frequency of 345i cm^{-1}, corresponding to a negative force constant for disrotatory cleavage of the long (1.971 Å) bond between C-2 and C-3. Conrotation of the two methylene groups was, in contrast, computed to have a positive force constant. The frequency for conrotatory torsion of the ring methylenes was calculated to be 507 cm^{-1}.

Unlike the $^2A_1$ σ state, the $^2B_1$ π state was found to have real frequencies for both disrotatory (732 cm^{-1}) and conrotatory (845 cm^{-1}) torsion of the ring methylene groups. The larger force constants for both vibrational modes in $^2B_1$, as well as the shorter (1.517 Å) bond length between C-2 and C-3 in this state than in $^2A_1$, are attributable to the fact that two electrons contribute to the bond between C-2 and C-3 in the $^2B_1$ π state, but only one electron contributes to this bond in the $^2A_1$ σ state.

Although the frequencies for methylene group torsion in $^2B_1$ were computed to be real, this state was found to have an imaginary frequency of 347i cm^{-1}, corresponding to torsion about the bond to the exocyclic methylene group. This result, which implies a twisted equilibrium geometry for the one-electron π bond in $^2B_1$, is not surprising, since twisted geometries are generally found for the one-electron π bonds in ethylenic radical cations.[23]

The geometry of the optimized C_2 structure for the lowest π state (^2B) of $MCP^{\bullet+}$ was found to have the exocyclic methylene group twisted from planarity by 20°. Twisting resulted in an energy lowering of only 0.2 kcal/mol with a UHF wave function and 1.1 kcal/mol at the MP2 level of theory. Since the energy lowering on methylene group twisting was found to be rather small, SD–CI calculations at the C_2 equilibrium geometry of the π state were not performed.

The geometries of the $^2B_1$ and $^2A_2$ states of planar $TMM^{\bullet+}$ were also optimized by UHF calculations with the 6-31G* basis set. However, RHF, UHF, MP2, and SD–CI calculations all failed to show the proper degeneracy between these two states at D_{3h} geometries, where they form the two components of $^2E''$. It was thus apparent that use of a more highly correlated wave function was essential to obtain the correct relative energies for these two states.

Previous experience with radicals[24] and diradicals[25] containing charged π systems has shown that CI wave functions which include all single σ excitations from all π configurations (ASSEFAPC) do not exhibit artifactual symmetry breaking and give correctly energetic degeneracies, which are required by symmetry.[15] Such CI wave functions, involving all possible excitations in the π space and all single excitations in the conceptual minimal basis set of σ orbitals, were generated for both $^2B_1$ and $^2A_2$ states. With the Dunning SV basis set, these ASSEFAPC CI calculations involved 23080 spin-adapted configurations for the former state and 22952 for the latter. The virtual orbitals were transformed to K orbitals in order to maximize the correlation provided by them.[26] At the optimized D_{3h} geometry these CI calculations gave energies of −154.6710 hartrees for $^2B_1$ and −154.6712 hartrees for $^2A_2$, which are degenerate to within about 0.1 kcal/mol.

These CI wave functions were then used to obtain the optimal CI geometries for $^2B_1$ and $^2A_2$ and the energies at these geometries. The C–H bond lengths and H–C–H bond angles were fixed at the values obtained from the 6-31G* UHF optimization for each state. The CI energy for each state was then calculated at different C–C bond lengths and C–C–C bond angles, and the energies were fitted to a quadratic potential function in these parameters. The optimized CI geometries for $^2B_1$ and $^2A_2$ that resulted are given in Table IV.

The C–C bond lengths at each geometry can be analyzed in terms of an e_y' Jahn–Teller distortion from D_{3h} symmetry. Such a distortion can be expressed as $\Delta r(2\mathbf{r}_4 - \mathbf{r}_2 - \mathbf{r}_3)/6^{1/2}$, where Δr measures the magnitude of the distortion from a D_{3h} geometry (where all the C–C bond lengths are equal to the average) and $\mathbf{r}_i$ is a vector pointing from the central carbon, C-1, to the peripheral carbon, C_i. For $^2B_1$ Δr = 0.026 Å from an average bond length of 1.433 Å, and for $^2A_2$ Δr = −0.021 Å from an average bond length of 1.431 Å.

For purely first-order Jahn–Teller effects the average bond lengths would be the same for both states, and the Δr values would be equal in magnitude, though opposite in sign. For example, the magnitudes of the Jahn–Teller-induced e_y' distortions of the C–C–C bond angles from 120° in both states are almost the same. The slightly larger magnitude of Δr for $^2B_1$ thus suggests that it is stabilized more than $^2A_2$ by higher-order Jahn–Teller effects.[15]

In fact, the ASSEFAPC CI energy of −154.6728 hartrees for $^2B_1$ is 0.0001 hartrees below that of $^2A_2$. Since $^2A_2$ is (spuriously) computed to be 0.0002 hartrees below $^2B_1$ at D_{3h} geometries, it seems likely that $^2B_1$ is actually the lower energy of the two states. Nevertheless, the more significant fact is that the CI energies at the equilibrium geometries of these two states are nearly identical. This finding indicates that the potential surface for pseudorotation between the three equivalent $^2B_1$ minima, via the $^2A_2$ saddle points that connect them,[15] is very flat. Therefore, as in the cyclopentadienyl radical,[27] where the potential surface for pseudorotation is also calculated to be quite flat,[28] it is likely that in the EPR spectrum of $TMM^{\bullet+}$ the unpaired electron will appear to have the same spin density on each peripheral carbon at all but the lowest temperatures.

(22) Binkley, J. S.; Pople, J. A.; Hehre, W. J. *J. Am. Chem. Soc.* **1980**, *102*, 939.
(23) See: Bellville, D. J.; Bauld, N. L. *J. Am. Chem. Soc.* **1982**, *104*, 294 and references therein.
(24) (a) Borden, W. T.; Davidson, E. R.; Feller, D. *J. Am. Chem. Soc.* **1981**, *103*, 5725. (b) Hrovat, D. A.; Borden, W. T. *Ibid.* **1985**, *107*, 8034.
(25) Borden, W. T.; Davidson, E. R.; Feller, D. *J. Am. Chem. Soc.* **1980**, *102*, 5302.
(26) Feller, D.; Davidson, E. R. *J. Chem. Phys.* **1981**, *74*, 3977.
(27) Liebling, G. R.; McConnell, H. M. *J. Chem. Phys.* **1965**, *42*, 3931.
(28) Borden, W. T.; Davidson, E. R. *J. Am. Chem. Soc.* **1978**, *101*, 3771.

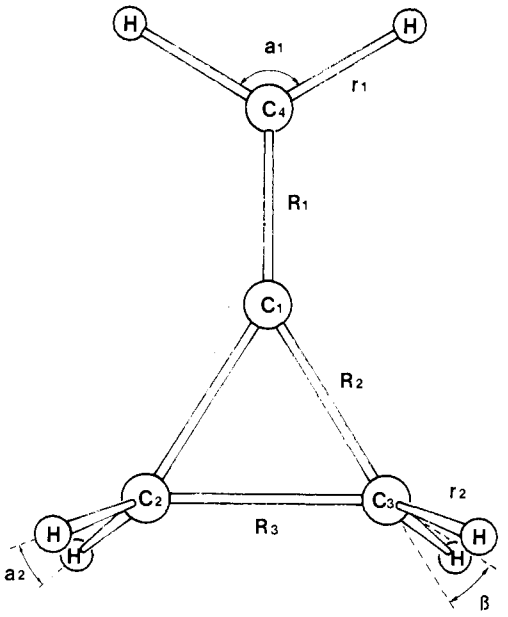

Figure 1. Geometrical parameters in MCP and MCP$^{\bullet+}$.

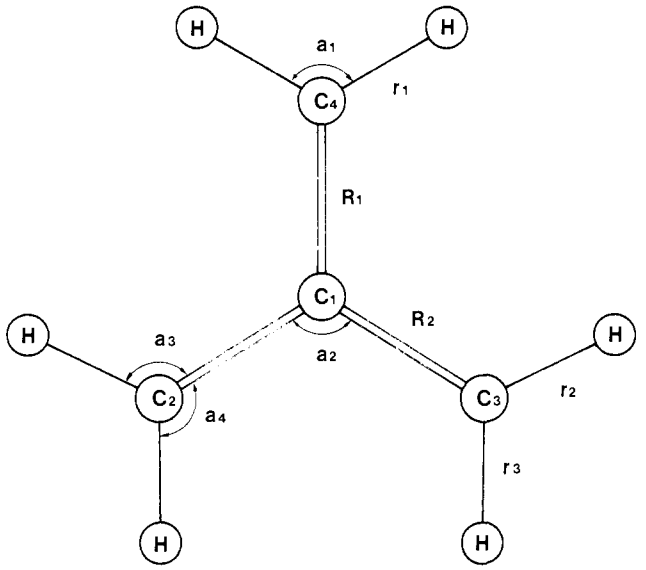

Figure 2. Geometrical parameters in planar and twisted TMM$^{\bullet+}$.

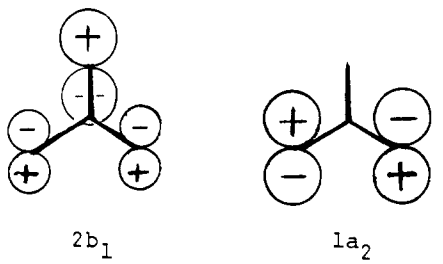

Figure 3. Degenerate (e″) nonbonding MOs of TMM.

The size of the Jahn–Teller effect in TMM$^{\bullet+}$ is, itself, rather small, resulting in rather modest changes in the C–C bond lengths and C–C–C bond angles and an energy lowering on distortion of only 1.1 kcal/mol. If one imagines TMM$^{\bullet+}$ being formed from the triplet ground state of TMM, the Jahn–Teller distortions of the C–C bond lengths and bond angles from the D_{3h} optimal geometry of triplet TMM can be understood on the basis of the nonbonding π orbital from which the electron is removed. These degenerate (e″) orbitals are shown schematically in Figure 3, where they are given their C_{2v} symmetry labels.

Removal of an electron from the $2b_1$ MO of triplet TMM gives the $^2A_2$ state of TMM$^{\bullet+}$. Since $2b_1$ is antibonding between the unique peripheral carbon (C-4) and the two equivalent carbons (C-2 and C-3) and bonding between C-2 and C-3, the C–C–C bond angle changes that result from removal of this electron are readily comprehensible. The opposite deviations of the C–C–C bond angles from 120° in $^2B_1$, which result from removal of an electron from $1a_2$, can be similarly understood. However, since both MOs have a node at the central carbon (C-1), the reason for the deviations of the C–C bond lengths from D_{3h} symmetry in the two low-lying states of TMM$^{\bullet+}$ is less obvious. Nevertheless, these bond length changes can also be understood on the basis of the nonbonding MOs pictured in Figure 3.

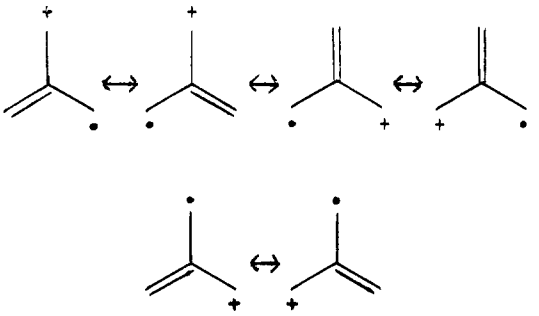

Figure 4. Resonance structures for TMM$^{\bullet+}$. A linear combination of the first four represents the bonding in $^2A_2$. A different linear combination of these four contributes to $^2B_1$, but the principal contributors to this state are the last two structures.

On removal of the electron from $2b_1$ in triplet TMM, a positively charged hole is created. This hole is largely localized at C-4; therefore the electrons in the bonding π MO ($1b_1$), particularly the electron in $1b_1$ that has spin opposite to the electron in $1a_2$, tend to become more localized at this carbon. This change strengthens the π bond between C-1 and C-4 and weakens the π bonds to C-2 and C-3 on going from triplet TMM to the $^2A_2$ state of TMM$^{\bullet+}$. The changes in π bonding that occur when the electron in $1a_2$ is ionized to form $^2B_1$ are explicable in a similar fashion.

Based on the foregoing discussion in terms of MO theory, it is easy to see why in valence bond theory the electronic structure of $^2A_2$ can be depicted by the first four resonance structures shown in Figure 4. A different linear combination of these four structures also contributes to $^2B_1$, but the principal resonance structures that contribute to the latter state are the last two in Figure 4. Consequently, it can be predicted that in neither electronic state of TMM$^{\bullet+}$ should rotation of the unique methylene group out of conjugation be favorable and that rotation of this group should be more difficult in $^2A_2$ than in $^2B_1$.

In order to test these two predictions and to compute the relative energies of the states of MCP$^{\bullet+}$ and TMM$^{\bullet+}$, we undertook additional calculations. Although planar MCP$^{\bullet+}$, TMM$^{\bullet+}$, and TMM$^{\bullet+}$ with one methylene group rotated out of conjugation all have C_{2v} symmetry, the number of electrons in π (b_1 and a_2) MOs is different in each of these species. Consequently, CI protocols, like the ASSEFAPC prescription employed for planar TMM$^{\bullet+}$, which treat σ and π electrons differently, cannot be used to calculate the relative energies of these three different species. Therefore, we computed their relative energies with UHF, RHF, MP2, and SD–CI calculations.

The UHF and MP2 calculations on the $^2B_1$ and $^2A_2$ states of planar TMM$^{\bullet+}$ were performed at the UHF-optimized 6-31G* geometries, whereas, the RHF and SD–CI calculations were performed at the CI-optimized SV geometries, given in Table IV. The two sets of geometries are quite similar, the only significant differences being in the slightly longer C–C bond lengths in the CI-optimized geometries. UHF vibrational analyses, performed with the 3-21G basis set at the optimized 3-21G geometry for each state, showed each to be a true minimum on the potential surface at this level of theory.

The energies calculated for the $^2B_1$ and $^2A_2$ states of planar TMM$^{\bullet+}$ are given in Table III. As discussed above, none of the calculations in Table III gives the proper D_{3h} degeneracy for these two states. Thus, it is not surprising that, unlike the ASSEFAPC

CI calculations, none of these less highly correlated wave functions gives the same energy for $^2B_1$ and $^2A_2$ at their equilibrium geometries. Even though the MP2 and SD–CI calculations give more nearly equal energies than do UHF or RHF, neither MP2 nor SD–CI contains sufficient π and σ–π electron correlation to predict the relative energies of these two states correctly. The differences of 5.5 (MP2) and 2.7 kcal/mol (SD–CI) between the energies of $^2B_1$ and $^2A_2$ provide an estimate of the errors in the relative energies in Table III that are caused by inadequacies in the treatment of electron correlation.

Also shown in Table III are the energies of the $^2B_2$ and $^2A_2$ states of $TMM^{\bullet+}$ with one methylene group twisted out of conjugation. The energies of the two low-lying states of this species were calculated at the geometries that were optimized with 6-31G* UHF calculations. The optimized geometries for the two states, which are given in Table IV, are rather similar. This is understandable, since the two states differ only in whether the unpaired electron occupies the nonbonding orbital of the twisted methylene group ($5b_2$) or of the allylic moiety ($1a_2$). The fact that the $1a_2$ MO of the allyl group, which is antibonding between C-2 and C-3, is empty in $^2B_1$ and singly occupied in $^2A_2$ accounts for the difference between the two states in the C–C–C bond angle of the allyl group.

The relative energies in Table III for planar and twisted $TMM^{\bullet+}$ show that, as anticipated, rotating the unique methylene group out of conjugation is unfavorable in both states of the planar molecule. Moreover, since the $^2A_2$ states of the planar and twisted radical cation correlate, the results in Table II also confirm that rotation of this methylene group from planarity is more difficult in $^2A_2$ than in $^2B_1$, which correlates with $^2B_2$ of twisted $TMM^{\bullet+}$.

On methylene group rotation from planarity, not only is more π bonding lost in $^2A_2$, but also all three electrons become localized in the same region of space, thus increasing the Coulomb repulsion energy between them. In contrast, in $^2B_1$ the loss of π bonding on twisting is smaller and is, in addition, partially compensated by localization of an electron on the twisted methylene group in $^2B_2$. This localization reduces the Coulomb repulsion energy on going from $^2B_1$ to $^2B_2$, since it confines the unpaired electron in the twisted radical cation to a region of space that is separate from that occupied by the remaining two π electrons.

Although methylene group rotation is predicted to be unfavorable in both low-lying states of the parent $TMM^{\bullet+}$, it could be argued that steric effects in the $TMM^{\bullet+}$ formed from **5** might make rotation of the substituted methylene group energetically favorable in the $^2B_1$ state of this radical cation. As discussed in the introduction, rotation of the substituted methylene group in the $TMM^{\bullet+}$ formed from **5** has been postulated in order to explain why back transfer of an electron does not lead to formation of any **6**.[8,9] However, it is also quite possible that significant rotation of the substituted methylene group occurs only after transfer of an electron back to the $TMM^{\bullet+}$, since it is well established that in the singlet state of the neutral TMM diradical this methylene group is twisted out of conjugation.[16]

The observation that **5** does not give **6** requires that, after ring opening of $\mathbf{5}^{\bullet+}$, the $TMM^{\bullet+}$ thus generated does not undergo closure to the isomeric $MCP^{\bullet+}$, $\mathbf{6}^{\bullet+}$. This requires that ring closure be either thermodynamically unfavorable or slow, relative to back electron transfer. The computational results contained in Table III show that, at least in the parent system, $TMM^{\bullet+}$ is thermodynamically more stable than either state of $MCP^{\bullet+}$.

The relative energies in Table III predict that opening of the $^2A_1$ σ state of $MCP^{\bullet+}$ to the $^2B_1$ state of planar $TMM^{\bullet+}$ should be exothermic by between 18.7 (MP2) and 17.0 kcal/mol (SD–CI). Since the ASSEFAPC CI calculations show that in planar $TMM^{\bullet+}$ $^2B_1$ has the same energy as $^2A_2$, the 13.2 (MP2) and 14.3 kcal/mol (SD–CI) energy differences between $^2A_1$ of $MCP^{\bullet+}$ and $^2A_2$ of $TMM^{\bullet+}$ provide an alternative estimate of the exothermicity of ring opening from $^2A_1$ of $MCP^{\bullet+}$.

In order for the $^2A_2$ and $^2B_1$ states of $TMM^{\bullet+}$ to have the same energy, the $^2A_2$ state of $TMM^{\bullet+}$ requires inclusion of more electron correlation than $^2B_1$. Neither MP2 nor SD–CI provide correlation for $^2A_2$ sufficient to make it degenerate with $^2B_1$.[29] Therefore, energy differences that are based on the MP2 or SD–CI energy of $^2B_1$ are likely to be more accurate than those based on the MP2 or SD–CI energy of $^2A_2$.

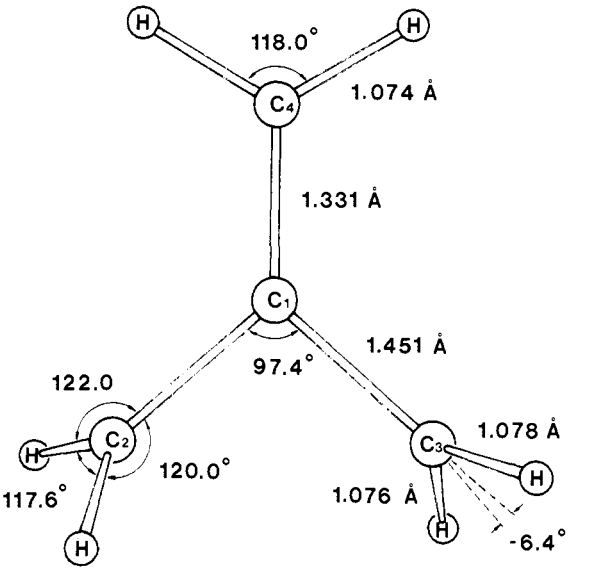

Figure 5. Conrotatory transition state connecting $^2A_1$ $MCP^{\bullet+}$ with $^2A_2$ $TMM^{\bullet+}$. The dihedral angle between the normal to the plane of the methylene groups and the plane containing the carbon atoms is 31.9°.

When the Davidson correction for quadruple excitations[30] is included, $^2A_2$ is calculated to be only 0.2 kcal/mol above $^2B_1$, in good agreement with the ASSEFAPC CI results. With the inclusion of the Davidson correction, the ring opening of the $^2A_1$ σ state of $MCP^{\bullet+}$ to the $^2B_1$ state of $TMM^{\bullet+}$ is computed to be exothermic by 16.3 kcal/mol.

Correcting for the difference in zero-point energies between the ring-closed $^2A_1$ state and the ring-opened $^2B_1$ state decreases the energy difference between these states by 1.1 kcal/mol. If the zero-point energy of the ring-opened $^2A_2$ state is used, the decrease is 0.8 kcal/mol. The net effect of applying both the zero-point and Davidson corrections is to decrease the CI estimate of the exothermicity of ring opening from the $^2A_1$ state of $MCP^{\bullet+}$ by 1.8 kcal/mol to 15.2 kcal/mol.

As discussed in the introduction, the disrotatory ring opening of $^2A_1$ to the $^2B_1$ state of $TMM^{\bullet+}$ is symmetry allowed, provided that the $^2A_1$ state of $MCP^{\bullet+}$ lies on the potential surface of lowest energy. This requires that at the equilibrium geometry of the $^2A_1$ σ state its energy be below that of the $^2B_1$ π state at the same geometry.[13] UHF and MP2 calculations confirmed that this is, in fact, the case. The computed vertical energy difference amounted to 28.3 kcal/mol at the former and 19.0 kcal/mol at the latter level of theory. The importance in $^2B_1$ of correlating the electron pair in the very long (1.971 Å) σ bond at the $^2A_1$ equilibrium geometry is responsible for the substantial decrease in the calculated energy difference on going from UHF to MP2.

As noted above, the vibrational analysis for the $^2A_1$ σ state of $MCP^{\bullet+}$ reveals a negative force constant, corresponding to the disrotatory mode of ring opening. Since this mode has a negative force constant and is symmetry allowed, there is every reason to believe ring opening of $^2A_1$ $MCP^{\bullet+}$ to $^2B_1$ $TMM^{\bullet+}$ is not only thermodynamically favorable but proceeds without an energy barrier in the disrotatory mode. Thus, assuming that the $MCP^{\bullet+}$ formed from **5** has a σ ground state, its opening to a $TMM^{\bullet+}$ is readily understandable.

(29) The unpaired electron occupies a more delocalized MO in $^2A_2$ than in $^2B_1$. Because the correct wavefunction for a delocalized electronic state requires inclusion of more electron correlation than does the wave function for a more localized state, the higher RHF, MP2, and SD–CI energies in Table III for $^2A_2$ than for $^2B_1$ are understandable. However, at the UHF level of theory electrons of opposite spin are allowed to have different spatial wave functions. This tends spuriously to favor the two $^2A_2$ wave functions, in which the unpaired electron occupies the a_2 MO. Note that the relative energies of the two $^2A_2$ wave functions are both computed to be about 10 kcal/mol too low at the UHF level of theory.

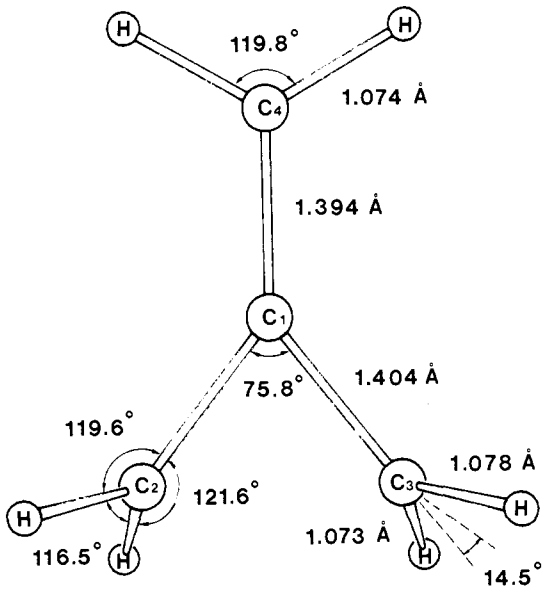

Figure 6. Disrotatory transition state connecting $^2B_1$ MCP$^{\bullet+}$ with $^2B_1$ TMM$^{\bullet+}$. The dihedral angle between the normal to the plane of the methylene groups and the plane containing the carbon atoms is 31.9°.

Conrotatory ring opening from $^2A_1$ of MCP$^{\bullet+}$ to $^2B_1$ of TMM$^{\bullet+}$ is also symmetry allowed, but there is apparently a barrier to this reaction since, as noted above, the force constant for methylene group conrotation in $^2A_1$ is found to be positive. We have located the transition state for conrotatory opening of $^2A_1$ by performing UHF calculations with the 6-31G* basis set. The transition state is depicted in Figure 5, and its energy is given in Table III.

A 3-21G vibrational analysis showed this geometry to have only one imaginary frequency of 760i cm^{-1}, corresponding to conrotation of C-2 and C-3. This confirms that it is the transition state for conrotatory ring opening. The zero-point energy of the transition state is 0.5 kcal/mol less than that of $^2A_1$, giving an estimated activation energy for this mode of ring opening of between 3.8 (MP2) and 3.3 kcal/mol (SD–CI with the Davidson correction for quadruple excitations).

Ring opening from the lowest π state of MCP$^{\bullet+}$ ($^2B_1$) is computed to be less exothermic than that from the lowest σ state ($^2A_1$). As shown in Table III, the calculated exothermicity of opening to $^2B_1$ of TMM$^{\bullet+}$ is 6.6 (MP2) and 6.5 kcal/mol (SD–CI). However, adding the zero-point (0.3 kcal/mol) and Davidson (1.3 kcal/mol) corrections to the SD–CI energy difference increases the calculated exothermicity to 8.1 kcal/mol.

Although the ring opening from the lowest π state of the parent MCP$^{\bullet+}$ is computed to be exothermic, the aryl substituents on the exocyclic double bond in **6**$^{\bullet+}$ could conceivably reverse the relative energies of the ring-closed and ring-opened forms of this radical cation. However, another possible explanation for the lack of ring opening observed in **6**$^{\bullet+}$ is that in the lowest π state, which is apparently the state formed from **6**,[9] ring opening is slow kinetically.

As noted above, although disrotatory ring opening of the $^2B_1$ π ground state of MCP$^{\bullet+}$ to the $^2B_1$ state of TMM$^{\bullet+}$ is orbital symmetry allowed, vibrational analysis shows that the lowest π state of the parent MCP$^{\bullet+}$ has a positive force constant for this torsional mode. Therefore, there must exist an energy barrier which separates this state from the $^2B_1$ state of TMM$^{\bullet+}$.

In order to determine the height of this barrier to ring opening in the parent MCP$^{\bullet+}$ we carried out a 6-31G* UHF optimization of the transition state that connects the $^2B_1$ states of the ring-closed and ring-opened radical cations along a disrotatory pathway. The optimized geometry is shown in Figure 6. A vibrational analysis showed it to have one imaginary vibrational frequency of 930i cm^{-1}, corresponding to methylene group disrotation. The energy at this geometry, computed by UHF, MP2, RHF, and SD–CI calculations, is given in Table III.

From the data in Table III, the activation energy for disrotatory ring opening of the $^2B_1$ ground state of MCP$^{\bullet+}$ to the $^2B_1$ state of TMM$^{\bullet+}$ via this transition state is 1.6 kcal/mol at the MP2 level of theory and 4.1 kcal/mol with SD–CI. Correction for differences in zero-point vibrational energy between the reactant and transition state reduces the activation energy by 0.6 kcal/mol.[31] Inclusion of the Davidson correction reduces the SD–CI activation energy by another 1.6 kcal/mol to a final value of 1.9 kcal/mol.

Although the energy of the transition state for disrotatory opening of MCP$^{\bullet+}$ is computed to be about 2 kcal/mol above that of the lowest π state, the energy of the transition state is substantially below that of the lowest σ state. As discussed above, both the σ and π state lie on the lowest potential surface for disrotatory ring opening. Consequently, both states of MCP$^{\bullet+}$ are connected to the $^2B_1$ state of TMM$^{\bullet+}$ by the same transition state. Since the transition state is computed to be lower in energy than the σ state of MCP$^{\bullet+}$, disrotatory ring opening from the σ state should proceed without activation.

Not surprisingly, the structure of the transition state for disrotatory ring opening resembles more closely that of the lower energy $^2B_1$ π state of MCP$^{\bullet+}$ than that of the higher energy $^2A_1$ σ state. In the transition state the length of the bond to the exocyclic methylene group is almost unchanged from that in $^2B_1$. Although the bond between C-2 and C-3 of the ring is lengthened to 1.725 Å, this is still considerably shorter than the 1.971 Å length of this bond in the σ state.

In contrast, the transition state for conrotatory ring opening resembles the $^2A_1$ σ state of MCP$^{\bullet+}$, both in the short bond to the exocyclic methylene group and in the long (2.181 Å) bond between C-2 and C-3. Again this is not surprising, since in the C_2 symmetry, which is maintained during conrotatory ring opening, the $^2A_1$ σ state of MCP$^{\bullet+}$ is ^2A, whereas, the $^2B_1$ π state is ^2B. Therefore, although these two states of MCP$^{\bullet+}$ use the same transition state for disrotatory ring opening, they use different transition states for conrotatory ring cleavage. The transition state shown in Figure 5 is ^2A and connects only the $^2A_2$ σ state of MCP$^{\bullet+}$ to the $^2A_1$ state of TMM$^{\bullet+}$. These states are orbitally correlated in C_2 symmetry.

In C_2 symmetry the $^2B_1$ π state of MCP$^{\bullet+}$ and the $^2B_1$ state of TMM$^{\bullet+}$ both have ^2B symmetry. However, a correlation diagram shows that the orbitals in these two states are not correlated. Consequently, conrotatory ring opening of the π state of MCP$^{\bullet+}$, being forbidden by orbital symmetry, is expected to encounter a sizable energy barrier.[12]

Because of the orbital crossing, the correct description of the transition state for conrotatory opening of $^2B_1$ is likely to require a multiconfigurational wave function. Therefore, we have made no attempt to locate this transition state. Nevertheless, since conrotatory ring opening of the $^2B_1$ π state is orbital symmetry forbidden, we are confident in predicting that ring opening of this state to the $^2B_1$ state of TMM$^{\bullet+}$ should occur by orbital symmetry allowed disrotation, which we calculate has an activation energy of only about 2 kcal/mol.

Since the activation energy for disrotatory ring opening of the π state is computed to be so small, it is somewhat surprising that the $^2B_1$ π state of the radical cation formed from **6** apparently does not undergo ring opening.[9] As mentioned above, a possible explanation is that the aryl substituents could, conceivably, cause ring opening in **6**$^{\bullet+}$ to become endothermic.

The CIDNP polarizations that are observed in **6** indicate formation of the π state of the radical cation, with a high degree of localization of the unpaired electron on the ring carbon, leaving the positive charge contained largely in the exocyclic diaryl-

(30) Davidson, E. R. In *The World of Quantum Chemistry*; Daudel, R., Pullman, B., Eds.; Dordrecht: The Netherlands, 1974.

(31) Since the torsion of the exocyclic methylene group has an imaginary frequency in $^2B_1$ MCP$^{\bullet+}$, it was not included in the calculation of the zero-point energy of this state. The small but finite value of this component of the zero-point energy of the π state at its equilibrium geometry, with the exocyclic methylene group twisted slightly from planarity, would partially cancel the very modest energy lowering that accompanies rotation of the exocyclic methylene group in this state.

methylene group.[9] In contrast, in the $^2B_1$ state of TMM$^{\bullet+}$, to which the π state of MCP$^{\bullet+}$ opens, the odd electron occupies the $2b_1$ nonbonding MO, which is largely localized on what was the exocyclic methylene group, and the positive charge is largely delocalized between C-2 and C-3. The necessity of moving the positive charge away from the diarylmethylene group in the ring opening of **6**$^{\bullet+}$ would certainly tend to make the reaction less exothermic in this substituted radical cation than in the parent MCP$^{\bullet+}$.[32]

The aryl substituents in **6**$^{\bullet+}$ should also tend to raise the activation energy for disrotatory ring opening. The existence of the $2b_1$ nonbonding MO in TMM$^{\bullet+}$ is what distinguishes the orbital symmetry allowed, disrotatory ring opening of the π state of MCP$^{\bullet+}$ from the symmetry-forbidden, disrotatory ring opening of the cyclopropyl radical, where the $2b_1$ orbital of the reactant becomes the antibonding $2b_1$ MO of the allyl radical.[12,33] The availability of $2b_1$ in TMM$^{\bullet+}$ thus makes the disrotatory ring opening of the lowest π state of MCP$^{\bullet+}$ very much like the analogous, orbital symmetry allowed reaction of the cyclopropyl cation.

To the extent that the aryl substituents in **6**$^{\bullet+}$ cause the π electron distribution in the lowest state of this radical cation to resemble that in the cyclopropyl radical more than that in the cyclopropyl cation, the activation energy for ring opening of **6**$^{\bullet+}$ should be greater than that of the parent MCP$^{\bullet+}$.

Conclusions

Our ab initio calculations on MCP$^{\bullet+}$ radical cation predict ring opening to TMM$^{\bullet+}$ to be exothermic from both the $^2B_1$ π ground state and the $^2A_1$ σ state of MCP$^{\bullet+}$. Disrotatory ring opening is computed to require an activation energy of about 2 kcal/mol from the π state but to proceed without activation from the σ state. Conrotatory ring opening of the π state is forbidden by orbital symmetry and, hence, is expected to require a much larger activation energy. Conrotatory opening of the σ state is allowed and is calculated to require an activation energy of about 4 kcal/mol. Therefore, ring opening is predicted to occur by a disrotatory pathway for both states.

ASSEFAPC CI calculations indicate that the $^2B_1$ and $^2A_2$ states of TMM$^{\bullet+}$ have nearly the same energy. Thus, pseudorotation in TMM$^{\bullet+}$ is predicted to be facile, and the EPR spectrum on TMM$^{\bullet+}$ should show all three methylene groups to be equivalent, except perhaps at very low temperatures. Rotation of one methylene group out of conjugation is computed to be unfavorable for both $^2B_1$ and $^2A_2$ but especially unfavorable for $^2A_2$.

Calculations have not been performed on the radical cations formed from **5** and **6**, which have been studied experimentally.[8-10] Nevertheless, the ring opening observed in **5**$^{\bullet+}$ is readily explicable if the aryl substituents on the ring confer a σ ground state on this radical cation. The TMM$^{\bullet+}$ radical cation formed from **5**$^{\bullet+}$ would not be expected to reclose to **6**$^{\bullet+}$, and back electron transfer to form the lowest singlet state of the neutral TMM should afford **5** instead of **6**, thus rationalizing the failure of **5** to form **6** after photoionization.

Finally, the failure of **6**$^{\bullet+}$ to undergo ring opening may be understood on the basis of the experimentally observed localization of the positive charge in the diarylmethylene group.[9] This type of localization is expected to make ring opening in the $^2B_1$ state of the corresponding TMM$^{\bullet+}$ less thermodynamically favorable than in the parent system. Moreover, localization of the unpaired electron on the ring carbon is anticipated to result in a higher activation energy for disrotatory ring opening in **6**$^{\bullet+}$ than in the parent MCP$^+$.

Acknowledgment. We thank the National Science Foundation for support of this research, including a generous allocation of time at the San Diego Supercomputer Center, where many of these calculations were carried out. Some of the calculations were performed on a Convex C-1 computer, whose purchase was made possible by a grant from the National Science Foundation.

Registry No. MCP$^{\bullet+}$, 109392-92-9; TMM$^{\bullet+}$, 57414-21-8.

(32) Of course, following disrotatory ring opening to $^2B_1$, pseudorotation of the TMM$^{\bullet+}$ to $^2A_2$ could occur. Pseudorotation from $^2B_1$ to $^2A_2$ should be thermodynamically favorable in the TMM$^{\bullet+}$ formed from 6$^{\bullet+}$, since the positive charge in $^2A_2$ is largely localized at the aryl-substituted methylene group.

(33) Longuet-Higgins, H. C. Abrahamson, E. W. *J. Am. Chem. Soc.* **1965**, *87*, 2045.

Reactions of Atomic Gold Ions with Aliphatic and Aromatic Hydrocarbons and Alkyl Halides

A. Kasem Chowdhury and Charles L. Wilkins*

Contribution from the Department of Chemistry, University of California, Riverside, California 92521. *Received November 24, 1986*

Abstract: The reactions of gold cations with aliphatic and aromatic hydrocarbons have been studied by using Fourier transform mass spectrometry. Hydride abstraction is the major reaction channel with alkanes larger than ethane. With larger alkanes, hydride abstraction by Au^+ generates internally excited alkyl cations which fragment in competition with collisional stabilization. A minor pathway involving C–H insertion followed by β-hydrogen migration leads to dehydrogenation. Generation of reactive gold carbene ($AuCH_2^+$) from methyl halides and methide and hydride abstraction studies allows estimation of lower limits for Au^+–CH_2, Au–CH_3, and Au–H bond dissociation energies ($D(Au^+–CH_2) \geq 95.0$ kcal/mol, $D(Au–CH_3) \geq 45.8$ kcal/mol, and $D(Au–H) > 67$ kcal/mol). Au^- undergoes slow S_N2 displacement reactions with methyl halides. With CCl_4 and $CHCl_3$, Au^- yields $AuCl_2^-$ ion, allowing estimation of the lower limit of bond dissociation energy, $D°(Au^–2Cl) \geq 162.6$ kcal/mol. Generation of $AuCBr_2^-$ from $CHBr_3$ appears to be the first observation of a gas-phase anionic metal carbene.

The challenge of understanding C–H and C–C bond activation by transition metals has prompted a great deal of interest in such reactions over the past several years. Development of novel ion sources[1,2] and new mass spectrometric techniques[3-5] have yielded a variety of fundamental thermodynamic, kinetic, and mechanistic information about gas-phase transition metal ion reactions.[7-11]

(1) Jones, R. W.; Staley, R. H. *J. Am. Chem. Soc.* **1982**, *104*, 1235–1238.

0002-7863/87/1509-5336$01.50/0